

# Shortcut To Adiabaticity for an Anisotropic Gas Containing Quantum Defects

D.J. Papoular and S. Stringari

*INO-CNR BEC Center and Dipartimento di Fisica, Università di Trento, 38123 Povo, Italy*

(Dated: June 16, 2021)

We present a Shortcut To Adiabaticity (STA) protocol applicable to 3D unitary Fermi gases and 2D weakly-interacting Bose gases containing defects such as vortices or solitons. Our protocol relies on a new class of exact scaling solutions in the presence of anisotropic time-dependent harmonic traps. It connects stationary states in initial and final traps having the same frequency ratios. The resulting scaling laws exhibit a universal form and also apply to the classical Boltzmann gas. The duration of the STA can be made very short so as to realize a quantum quench from one stationary state to another. When applied to an anisotropically trapped superfluid gas, the STA conserves the shape of the quantum defects hosted by the cloud, thereby acting like a perfect microscope, which sharply contrasts with their strong distortion occurring during the free expansion of the cloud.

PACS numbers: 67.85.-d, 05.30.-d, 67.85.De

Solitons and quantized vortices are fundamental excitations of non-linear media and play a key role in superfluid dynamics [1]. In anisotropic geometries, the energetically favored defects are solitonic vortices, characterized by a non-circular velocity field which nevertheless presents non-zero circulation [2, 3]. The investigation of their dynamics has been initiated by recent experiments where they were created either deterministically by phase imprinting [4], or spontaneously in a system which is quickly driven through a phase transition [5]. These defects exhibit intricate dynamics and decay mechanisms. For example, the snake instability [6], which affects solitons in 2D and in 3D, can lead to the creation of a solitonic vortex, a process which is likely to have played a role in [7]. The size of these defects is set by the healing length [8, chap. 5], which is too small to allow for in-situ observation. Up to now they have always been observed after the free expansion of the cloud, which increases the core dimensions. However, in the anisotropic case, the free expansion strongly distorts the cloud, and its use in the presence of a solitonic vortex leads to an involved density profile sporting a twisted nodal line [9].

An alternative to free expansion is provided by the recent Shortcut To Adiabaticity (STA) schemes [10, 11], which reversibly evolve a many-body system from one state to another, reaching the same target state as an adiabatic transformation in a much shorter time over which decoherence and losses are minimal. They allow for the manipulation of the momentum spread of a wavepacket without the time constraints of delta kick cooling [12, 13]. They can be formulated as counterdiabatic driving [14, 15]. They are being considered for the preparation of many-body states [16–18], they have motivated an exploration of the quantum speed limit [19] and reflection on the third law of thermodynamics [20].

The construction of an STA relies on the existence of a scaling solution to the equation describing the many-body dynamics of the system in a time-dependent trap. Such a solution exists for the ideal gas in a harmonic trap

and has been used to construct an STA solution [10] implemented experimentally on a Bose cloud above  $T_c$  [21]. Allowing for interactions, a scaling solution exists for the hydrodynamic equations holding in the Thomas-Fermi regime [22–24] and the corresponding STA [25] has been realized experimentally [26]. Scaling solutions also exist for a class of many-body systems including interacting quasi-1D Bose gases [27, 28], and for box potentials [29].

Up to now, STAs have been demonstrated either in the ideal-gas or the Thomas-Fermi regimes. Their application to a gas containing defects requires going beyond these approximations, as their existence and dynamics result from the interplay between quantum pressure and interactions. Harmonically-trapped 2D weakly-interacting Bose gases and 3D unitary Fermi gases are specially promising. In the isotropic case, they allow for an exact scaling solution to the many-body dynamics [22, 30] requiring no time-dependent manipulation of the interactions [31], due to a dynamical symmetry shared by the 2D bosonic [32, 33] and 3D fermionic [30] gases, as well as by the classical Boltzmann gas [34]. The absence of damping of the breathing mode due to this symmetry has been confirmed experimentally in the Bose case [35].

In this Letter, we introduce a novel STA protocol applicable to anisotropic 2D Bose gases and 3D unitary Fermi gases hosting defects, as well as to classical Boltzmann gases. Our STA links two stationary states in initial and final traps with the same anisotropy. It allows for a reversible and arbitrarily fast compression or expansion of the cloud which conserves the aspect ratios and acts as a homothety on the defects. This sharply contrasts with the free expansion of the anisotropic cloud, which leads to a time-dependent aspect ratio and an inversion of the cloud anisotropy, and dramatically affects the density and phase profiles of vortices [9] (see Fig. 1C). Our STA can be used to quench the cloud [36] from one anisotropic stationary state to another. It relies on a new and exact scaling solution for the dynamics of the cloud in a time-dependent anisotropic harmonic trap. Exact solu-

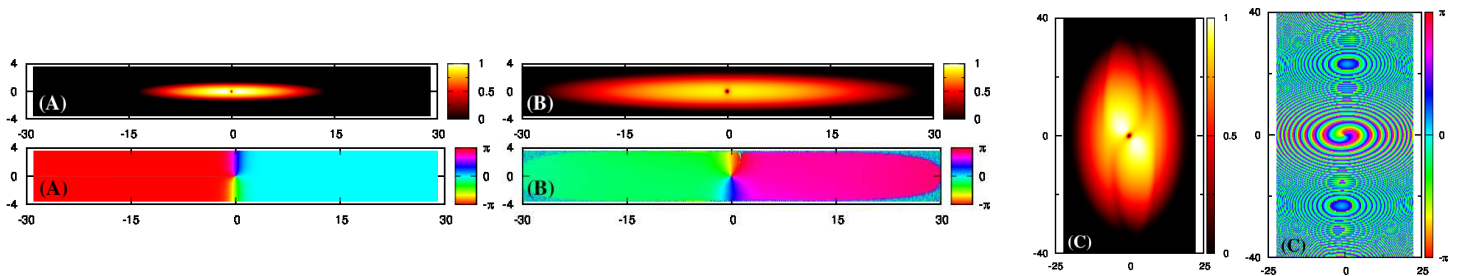


FIG. 1. (A) Density (top) and phase (bottom) profiles for an initial anisotropic Bose cloud containing a vortex ( $\omega_{02}/\omega_{01} = 10$  and  $m g_{2D} N/\hbar^2 = 3100$ , corresponding to the chemical potential  $\mu_{2D}/\hbar\omega_{01} \approx 100$ ). (B) Density and phase profiles after the STA evolution represented on Fig. 2A, at the time  $\omega_{01}t = 1.8$ . (C) Density and phase profiles after the free expansion of the same initial cloud during the same time ( $\omega_{01}t = 1.8$ ). All six plots result from a numerical solution of Eq. (3) in imaginary time (left) and real time (center, right). Lengths are in units of  $(\hbar/m\omega_{01})^{1/2}$  and densities are normalized to the maximum density.

tions for the dynamics of quantum systems are rare, and we believe ours to be the first analytical solution describing the dynamics of a quantum gas in a time-dependent anisotropic trap. It is applicable if the spatial aspect ratio of the cloud remains constant in time, though the ratios of the trapping frequencies need not be constant.

*Scaling solution for 3D anisotropic Fermi gases.* — We consider a 3D unitary Fermi gas in the harmonic trap  $V(\mathbf{r}, t) = m \sum_{j=1}^D \omega_j^2(t) x_j^2/2$ , where  $m$  is the atomic mass and  $D = 3$  is the number of spatial dimensions. Note that  $V(\mathbf{r}, t)$  is both time-dependent and anisotropic. We describe the system dynamics using the Schrödinger equation applied to  $N$ -particle wavefunctions  $\Psi(\mathbf{R})$ , where  $\mathbf{R} = (\mathbf{r}_1, \dots, \mathbf{r}_N)$  is the set of all particle coordinates. Interactions are included through the Bethe–Peierls (BP) boundary conditions [30]. We assume that, for  $t \leq 0$ ,  $\Psi$  is a stationary state (which need not be the ground state and may host a defect, e.g., a quantized vortex) in the constant trap  $V_0(\mathbf{r}) = m \sum_{j=1}^D \omega_{0j}^2 x_j^2/2$ . We seek a solution to the Schrödinger equation of the form [30]:

$$\Psi(\mathbf{R}, t) = \frac{e^{-iE\tau/\hbar}}{b^{ND/2}} \exp\left[\frac{imb}{2\hbar b} R^2\right] \Psi(\mathbf{R}/b, 0), \quad (1)$$

where  $b(t)$  is the only scaling parameter, and  $\tau(t) = \int^t dt' b^2(t')$  is the reduced time. The positive function  $b(t)$  satisfies the boundary conditions  $b(0) = 1$ ,  $\dot{b}(0) = 0$ ,  $\ddot{b}(0) = 0$ , where the dots denote derivation with respect to the time  $t$ . We find that, if the trap frequencies satisfy:

$$\omega_j^2(t) = \frac{\omega_{0j}^2}{b^4} - \frac{\ddot{b}}{b} \quad \text{for } 1 \leq j \leq D, \quad (2)$$

then Eq. (1) is an exact solution of the Schrödinger equation for  $t > 0$ . If  $\omega_{01} = \omega_{02} = \omega_{03}$ , our solution reduces to the isotropic solution of Ref. [30]. In the general case, the scaling parameter  $b(t)$  being equal along all spatial directions follows from the requirement that Eq. (1) conserve the BP conditions. As we shall show below, the condition on the  $\omega_j^2(t)$ 's for the anisotropic scaling solution to hold (Eq. 2) is the same for all three considered systems

(Fermi, Bose, and Boltzmann gases), and follows from their shared dynamical symmetry. A remarkable feature of the unitary Fermi gas is that the same scaling solution applies to all eigenstates of the Hamiltonian satisfying the BP conditions, and thus holds at all temperatures.

The scaling transformation  $\Psi(\mathbf{R}/b, 0)/b^{ND/2}$  in Eq. (1) dictates the two accompanying phase factors. The first term, proportional to  $\tau$ , represents the evolution with the rescaled time  $\tau$  of the phase of a stationary state. The second one, proportional to  $R^2$ , is a gauge transform following from the continuity equation. The joint rescaling of the space and time coordinates, along with this gauge transform, allow us to describe the dynamics of the system exactly using the differential equations of Eq. (2). In particular, Eq. (1) shows that all mean-squared radii of the gas satisfy  $\langle x_i^2(t) \rangle / \langle x_i^2 \rangle_0 = b^2(t)$ , where the average  $\langle x_i^2 \rangle_0$  relates to the stationary configuration for  $t \leq 0$ .

*2D Bose gas* — We consider a Bose gas which is tightly confined in the direction  $z$ , and trapped in the harmonic potential  $V(\mathbf{r}, t) = m(\omega_1^2(t)x^2 + \omega_2^2(t)y^2)/2$  in the directions  $x$  and  $y$ . We assume that the oscillator length  $l_z$  for the axial confinement is both larger than the scattering length  $a_{3D}$  characterizing 3D collisions and smaller than the healing length. The first assumption ensures that the scattering amplitude is momentum-independent and that the quantum depletion is negligible, hence avoiding the quantum anomaly affecting the scale invariance of 2D systems [37–39], while the second means that the atomic density does not spill beyond the axial ground state [40]. These experimentally realistic conditions [41] allow for a description of the  $T = 0$  dynamics of the system using the 2D Gross–Pitaevskii equation (GPE) [8, chap. 17]:

$$i\hbar \frac{\partial \Phi}{\partial t} = -\frac{\hbar^2}{2m} \Delta \Phi + V(\mathbf{r}, t)\Phi + g_{2D}|\Phi|^2\Phi, \quad (3)$$

where  $\Phi(\mathbf{r}, t)$  is the Bose order parameter and the Laplacian  $\Delta = \partial_x^2 + \partial_y^2$ . The coupling constant  $g_{2D}$ , satisfying  $g_{2D}m/\hbar^2 = \sqrt{8\pi}a_{3D}/l_z$  [42], should be small for the logarithmic corrections to the equation of state to be negligible [43] and, hence, to avoid the quantum anomaly

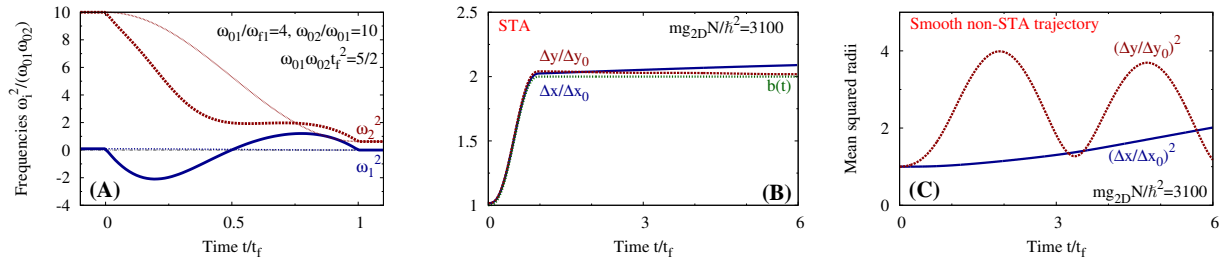


FIG. 2. (A) Thick lines: Squared trapping frequencies which achieve an anisotropic STA linking the stationary states in two 2D traps with  $\omega_{02}/\omega_{01} = \omega_{f2}/\omega_{f1} = 10$  and  $\omega_{01}t_f = 0.5$ . Thin lines: smooth non-STA trajectory. (B) Comparison between the expected scaling parameter and the calculated quadratic mean radii  $\Delta x = \sqrt{\langle x^2(t) \rangle}$  and  $\Delta y = \sqrt{\langle y^2(t) \rangle}$  for the STA trajectory starting from the initial cloud of Fig. 1(left) for times up to  $t/t_f = 6$  (i.e.  $\omega_{01}t = 3$ ). (C) Quadratic mean radii for the non-STA trajectory of panel (A). The graphs (B) and (C) result from a numerical solution of the GP Eq. (3) with  $mg_{2D}N/\hbar^2 = 3100$ .

discussed above. If  $\omega_{1,2}$  fulfill Eq. (2), then the order parameter  $\Phi(\mathbf{r}, t)$  in Eq. (3) obeys the same scaling law Eq. (1) as the unitary Fermi gas, with  $D = 2$  and  $N = 1$ . The spatial aspect ratio  $\mathcal{R} = \sqrt{\langle y^2 \rangle / \langle x^2 \rangle}$  of the cloud is constant in time, even though the frequency ratio  $\omega_2(t)/\omega_1(t)$  depends on time (Eq. 2). If  $\omega_{01} = \omega_{02}$ , our solution reduces to the known isotropic solution [22].

*Boltzmann gas* — We finally describe the classical Boltzmann gas through its distribution function  $f(\mathbf{r}, \mathbf{v}, t)$  governed by the Boltzmann equation [44, chap. 2]:

$$\partial_t f + \mathbf{v} \cdot \nabla_{\mathbf{r}} f + \frac{\mathbf{F}}{m} \cdot \nabla_{\mathbf{v}} f = I_{\text{coll}}[f], \quad (4)$$

where  $\mathbf{F} = -\nabla_{\mathbf{r}} V$  is the external force, and  $I_{\text{coll}}[f]$  is the collisional integral. We seek an  $f(\mathbf{r}, \mathbf{v}, t)$  of the form:

$$f = \exp \left[ -m\beta \left( \frac{\beta_0^2}{\beta^2} \sum_{i=1}^D \omega_{0i}^2 x_i^2 + (\mathbf{v} - \dot{\beta} \mathbf{r} / 2\beta)^2 \right) \right], \quad (5)$$

where  $\beta$  is the inverse temperature and  $\beta_0$  is its stationary  $t < 0$  value. If the  $\omega_i$ 's satisfy Eq. (2) with  $b = (\beta/\beta_0)^{1/2}$ , then  $f$  is an exact solution of the Boltzmann Eq. (4). The presence of a single scaling parameter reflects the equality of temperature along all spatial directions. In the isotropic case, Eq. (5) reduces to the solution of Ref. [34].

*Shortcut to adiabaticity* — We now use the scaling solution described above to explicitly construct an STA transforming the initial stationary state into another stationary state in a trap with the same frequency ratios, i.e.  $\omega_{fi}/\omega_{fj} = \omega_{0i}/\omega_{0j}$ . The  $\omega_{fj}$ 's describe the final state, reached at the time  $t_f$  which is chosen at will. In analogy with the isotropic scheme of Ref. [34], we first choose an appropriate time dependence for  $b(t)$ , and then deduce the time-dependent frequencies  $\{\omega_j(t)\}$ . We take  $\omega_j(t \geq t_f) = \omega_{fj}$ , and require that  $\Psi(\mathbf{r}, t)$  be stationary for  $t \geq t_f$ , i.e.  $\dot{b}(t_f) = 0$  and  $\ddot{b}(t_f) = 0$ . Combined with Eq. (2), the latter condition defines the value  $b_f = b(t_f)$ :

$$\frac{\omega_{fj}}{\omega_{0j}} = \frac{1}{b^2(t_f)} \quad \text{for } 1 \leq j \leq D. \quad (6)$$

Provided that Eq. (6) holds, the scaling parameter  $b(t)$  must satisfy 3 boundary conditions for  $t = 0$  and 3 others for  $t = t_f$  [45]. Numerous choices are possible for  $b(t)$ , the simplest being the following fifth-order polynomial:

$$b(t) = 1 + (b_f - 1) \left[ 10 \left( \frac{t}{t_f} \right)^3 - 15 \left( \frac{t}{t_f} \right)^4 + 6 \left( \frac{t}{t_f} \right)^5 \right]. \quad (7)$$

Once  $b(t)$  is known, the frequencies  $\omega_j(t)$  achieving the STA are determined using Eq. (2). Their evolution in time does not depend on the interaction strength or the atom number. For given values of  $m$  and  $a_{3D}$ , the STA trajectory  $\{\omega_j^2(t)\}$  depends on three parameters. First, the scaled duration  $(\prod \omega_{0j})^{1/D} t_f$  determines the attractive or repulsive nature of the trapping frequencies: shorter  $t_f$ 's require repulsive potentials ( $\omega_j^2 < 0$ ) for longer fractions of the total time. Second, the ratio  $\omega_{01}/\omega_{f1}$  sets the final cloud dimensions (Eq. 6). Third, the ratios  $\omega_{0i}/\omega_{0j}$  ( $i < j$ ) set the time-independent spatial aspect ratios  $\mathcal{R}_{ij} = [\langle x_j^2 \rangle / \langle x_i^2 \rangle]^{1/2}$ . Our exact solution holds for all coupling strengths from the ideal gas ( $\mathcal{R}_{ij} = (\omega_{0i}/\omega_{0j})^{1/2}$ ) to the Thomas-Fermi regime ( $\mathcal{R}_{ij} = \omega_{0i}/\omega_{0j}$ ). For  $t \geq t_f$ ,  $\Psi(\mathbf{r}, t)$  is stationary and its time evolution simply leads to a phase linear in  $(t - t_f)$ .

We now demonstrate this new STA protocol on the expansion of an anisotropic 2D Bose cloud containing a single vortex (Figs. 1 and 2). The single-vortex state is a stationary state of Eq. (3). It is the lowest-energy state satisfying the symmetry conditions  $\Psi(-x, -y, t) = -\Psi(x, y, t)$  and  $\Psi(-x, y, t) = \Psi^*(x, y, t)$ . Imposing these conditions on the initial wavefunction allows for its calculation using imaginary-time evolution despite the absence of any gauge or rotation term in Eq. (3). We start from the single-vortex stationary state with  $\omega_{02} = 10\omega_{01}$  and  $mgN/\hbar^2 = 3100$ , whose density and phase profiles are represented on Fig. 1 (left, top and bottom). Over the short time  $\omega_{01}t_f = 1/2$ , the STA trajectory reaches a new stationary state where both trapping frequencies are four times as small as their initial values. Figure 2A shows  $\omega_{1,2}^2(t)$  for  $0 \leq t \leq t_f$ . The exact prediction for the scal-

ing parameter  $b(t)$  (Eq. (7)) is compared on Fig. 2B to the calculated values for the ratio  $\Delta x/\Delta x_0 = \Delta y/\Delta y_0$  characterizing the mean radii of the cloud, obtained through a numerical solution of the GPE Eq. (3) for times up to  $t = 6t_f = 3/\omega_{01}$ . The density and phase profiles of the cloud at  $t = 3.6t_f$ , shown on Fig. 1 (center), are those of a stationary anisotropic vortex in the expanded trap. The small residual oscillations seen on Fig. 2B for  $t \gtrsim t_f$ , which start before  $t_f$  and survive for longer times, are an artefact of the numerical simulation, and their amplitude decreases with increasing resolutions of the spatial grid.

The above results illustrate three important properties of our STA protocol. First, the  $\omega_j^2$ 's determined by Eq. (2) can be transiently negative, corresponding to an expulsive potential, as already noted in Ref. [34]. Second, despite the initial and final trap anisotropies being the same, the ratio  $\omega_2^2(t)/\omega_1^2(t)$  is not constant in time. Indeed, Fig. 2A shows that  $\omega_2^2(t) > 0$  at all times whereas  $\omega_1^2(t)$  is negative for intermediate times, which is a dramatic consequence of anisotropy. Third, the  $\omega_j^2$ 's are continuous at  $t = 0$  and  $t = t_f$ , but they need not go smoothly to the initial and final values, as long as  $b(t)$  satisfies the correct boundary conditions. By contrast, even a very smooth non-STA trajectory linking the initial and final states within the same time  $t_f$  results in large-amplitude oscillations of the cloud radii for  $t > t_f$  (Fig. 2C). The discontinuity in the derivatives of  $\omega_{1,2}^2$  at  $t = 0$  and  $t_f$  follows from our choice for  $b(t)$  (Eq. 7), and can be avoided by choosing a higher-order polynomial.

The stationary behavior of the cloud following an STA (Fig. 2B) sharply contrasts with its behavior during free expansion, which leads to a time-dependent aspect ratio and an inversion of the cloud anisotropy for all interaction strengths (Fig. 3). Unlike the STA, the free expansion from an anisotropic trap is not governed by a single scaling parameter and cannot be formulated in a universal way. In particular, the scaling parameters  $b_j$ , characterizing the dilation along the spatial directions  $1 \leq j \leq D$ , obey different equations in the ideal gas and the hydrodynamic regimes. For the 2D ideal Bose gas at  $T = 0$ , the scaling law reads  $\ddot{b}_j = \omega_{0j}^2/b_j^3$ . Instead, in the hydrodynamic regime, it reads  $\ddot{b}_j = \omega_{0j}^2/(b_j b_x b_y)$  for the 2D Bose gas and  $\ddot{b}_j = \omega_{0j}^2/[b_j (b_x b_y b_z)^{2/3}]$  for the 3D unitary Fermi gas [46]. Only in the case of isotropic trapping do the above laws take the universal form  $\ddot{b} = \omega_0^2/b^3$  which, by the way, coincides with Eq. (2) after setting  $\omega_{0j} = \omega_0$  and  $\omega_j(t) = 0$  for  $t > 0$ . The anisotropy of the hydrodynamic scaling laws leads to a peculiar change in the shape of the expanding density profiles, which was experimentally observed in [47] with a unitary Fermi gas.

Comparing the density and phase profiles obtained from the initial cloud containing a vortex and undergoing an STA (Fig. 1B) or free expansion (Fig. 1C) confirms that the STA acts as a homothety on the vortex, whereas free expansion yields the twisted nodal line characteriz-

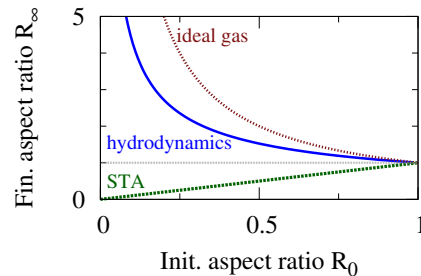


FIG. 3. Final aspect ratio  $\mathcal{R}_\infty$  of the anisotropic cloud as a function of the initial value  $\mathcal{R}_0$ , for the hydrodynamic (solid blue) and ideal-gas ( $\mathcal{R}_\infty = 1/\mathcal{R}_0$ , dotted brown) free expansions, and for an STA evolution ( $\mathcal{R}_\infty = \mathcal{R}_0$ , dashed green).

ing soliton vortices [9]. The free expansion of a gas is practically irreversible. On the contrary, the time reversal of an STA leads to another STA which performs the inverse transformation. More precisely, if  $\{\omega_j(t)\}$  is an STA satisfying Eq. (2) with the scaling parameter  $b(t)$ , then  $\{\omega_j(t_f - t)\}$  is an STA for the scaling function  $\bar{b}(t) = b(t_f - t)/b_f$ . Thus, an STA compressing the cloud is obtained by time-reversing the trajectory of Fig. 2A.

The duration  $t_f$  of the STA can be arbitrarily small. Therefore, the STA does not exhibit any quantum speed limit [48]. If  $\omega_{f1}/\omega_{01}$  is sufficiently small,  $b_f$  can be made large (Eq. (6)). Hence, the cloud can be expanded to an arbitrarily large radius within an arbitrarily small time, thus realizing a quantum quench from one stationary state to another, with the caveat that the expulsive part of the trajectory ( $\omega_j^2 < 0$ ) becomes more pronounced.

In conclusion, our exact scaling solution for Fermi, Bose, and Boltzmann gases is an important step towards the analytical description of the dynamics of anisotropic systems. The experimental demonstration of the dynamical SO(2,1) symmetry has so far remained elusive in 3D geometries, where isotropic traps are challenging to achieve, and the application of our STA to an anisotropic 3D Fermi gas will provide its experimental signature. Quasi-2D Bose gases are readily created and manipulated experimentally [41], and the required anisotropic (trapping or expulsive) potentials can be obtained by combining red- and blue-detuned optical potentials [49]. Our protocol will allow for a detailed experimental investigation of the dynamics and decay mechanisms of defects in anisotropic clouds [4, 7]. For instance, the cloud can be cooled and condensed in a strongly-confining trap where evaporative cooling is efficient, and then quickly expanded using the STA, without any distortion, into a weakly-confining trap where defects are easier to observe.

We are grateful to L. Pitaevskii, Y. Castin, G. Lamporesi, and H. Perrin for fruitful discussions. This work has been supported by ERC through the QGBE grant.

- 
- [1] P. G. Kevrekidis, D. J. Frantzeskakis, and R. Carretero-González, eds., *Emergent non-linear phenomena in Bose-Einstein condensates* (Springer, 2008).
- [2] J. Brand and W. P. Reinhardt, *Phys. Rev. A* **65**, 043612 (2002).
- [3] A. Muñoz Mateo and J. Brand, *Phys. Rev. Lett.* **113**, 255302 (2014).
- [4] M. J. H. Ku, W. Ji, B. Mukherjee, E. Guardado-Sanchez, L. W. Cheuk, T. Yefsah, and M. W. Zwierlein, *Phys. Rev. Lett.* **113**, 065301 (2014).
- [5] G. Lamporesi, S. Donadello, S. Serafini, F. Dalfovo, and G. Ferrari, *Nat. Phys.* **9**, 656 (2013).
- [6] Z. Dutton, M. Budde, C. Slowe, and L. V. Hau, *Science* **293**, 663 (2001).
- [7] S. Donadello, S. Serafini, M. Tylutki, L. P. Pitaevskii, F. Dalfovo, G. Lamporesi, and G. Ferrari, *Phys. Rev. Lett.* **113**, 065302 (2014).
- [8] L. Pitaevskii and S. Stringari, *Bose-Einstein Condensation* (Oxford University Press, 2003).
- [9] M. Tylutki, S. Donadello, S. Serafini, L. P. Pitaevskii, F. Dalfovo, G. Lamporesi, and G. Ferrari, arXiv:1410.5475 (2014).
- [10] X. Chen, A. Ruschhaupt, S. Schmidt, A. delCampo, D. Guéry-Odelin, and J. G. Muga, *Phys. Rev. Lett.* **104**, 063002 (2010).
- [11] E. Torrontegui, S. Ibez, S. Martínez-Garaot, M. Modugno, A. del Campo, D. Guéry-Odelin, A. Ruschhaupt, X. Chen, and J. G. Muga, in *Advances in Atomic, Molecular, and Optical Physics*, Vol. 62 (Academic Press, 2013) pp. 117 – 169.
- [12] H. Ammann and N. Christensen, *Phys. Rev. Lett.* **78**, 2088 (1997).
- [13] T. Aoki, T. Kato, Y. Tanami, and H. Nakamatsu, *Phys. Rev. A* **73**, 063603 (2006).
- [14] A. del Campo, *Phys. Rev. Lett.* **111**, 100502 (2013).
- [15] S. Deffner, C. Jarzynski, and A. del Campo, *Phys. Rev. X* **4**, 021013 (2014).
- [16] A. del Campo, *Phys. Rev. A* **84**, 031606(R) (2011).
- [17] A. del Campo, M. M. Rams, and W. H. Zurek, *Phys. Rev. Lett.* **109**, 115703 (2012).
- [18] S. Campbell, G. De Chiara, M. Paternostro, G. Palma, and R. Fazio, arXiv:1410.1555 (2014).
- [19] M. G. Bason, M. Viteau, N. Malossi, P. Huillery, E. Arimondo, D. Ciampini, R. Fazio, V. Giovanetti, R. Mannella, and O. Morsch, *Nature Phys.* **8**, 147 (2012).
- [20] A. Levy and R. Kosloff, *Phys. Rev. Lett.* **108**, 070604 (2012).
- [21] J. F. Schaff, X. L. Song, P. Vignolo, and G. Labeyrie, *Phys. Rev. A* **82**, 033430 (2010).
- [22] Y. Kagan, E. L. Surkov, and G. V. Shlyapnikov, *Phys. Rev. A* **54**, R1753 (1996).
- [23] Y. Castin and R. Dum, *Phys. Rev. Lett.* **77**, 5315 (1996).
- [24] Y. Kagan, E. L. Surkov, and G. V. Shlyapnikov, *Phys. Rev. A* **55**, R18 (1997).
- [25] J. Muga, X. Chen, A. Ruschhaupt, and D. Guery-Odelin, *J. Phys. B* **42**, 241001 (2009).
- [26] J.-F. Schaff, X.-L. Song, P. Capuzzi, P. Vignolo, and G. Labeyrie, *EPL* **93**, 23001 (2011).
- [27] V. Gritsev, P. Barmettler, and E. Demler, *New J. Phys.* **12**, 113005 (2010).
- [28] W. Rohringer, D. Fischer, F. Steiner, I. Mazets, J. Schmiedmayer, and M. Trupke, arXiv:1312.5948 (2013).
- [29] A. del Campo and M. G. Boshier, *Sci. Rep.* **2**, 648 (2012).
- [30] Y. Castin and F. Werner, in *The BCS-BEC Crossover and the Unitary Fermi Gas* (Springer, 2012).
- [31] A. del Campo, *Europhys. Lett.* **96**, 60005 (2011).
- [32] L. P. Pitaevskii, *Phys. Lett. A* **221**, 14 (1996).
- [33] L. P. Pitaevskii and A. Rosch, *Phys. Rev. A* **55**, R853 (1997).
- [34] D. Guery-Odelin, J. G. Muga, M. J. Ruiz-Montero, and E. Trizac, *Phys. Rev. Lett.* **112**, 180602 (2014).
- [35] F. Chevy, V. Bretin, P. Rosenbusch, K. W. Madison, and J. Dalibard, *Phys. Rev. Lett.* **88**, 250402 (2002).
- [36] A. Polkovnikov, K. Sengupta, A. Silva, and M. Vengalattore, *Rev. Mod. Phys.* **83**, 863 (2011).
- [37] M. Olshanii, H. Perrin, and V. Lorent, *Phys. Rev. Lett.* **105**, 095302 (2010).
- [38] Y. Hu and Z. Liang, *Phys. Rev. Lett.* **107**, 110401 (2011).
- [39] J. Hofmann, *Phys. Rev. Lett.* **108**, 185303 (2012).
- [40] K. Merloti, R. Dubessy, L. Longchambon, M. Olshanii, and H. Perrin, *Phys. Rev. A* **88**, 061603 (2013).
- [41] Z. Hadzibabic and J. Dalibard, *Riv. Nuovo Cimento* **34**, 389 (2011).
- [42] D. S. Petrov and G. V. Shlyapnikov, *Phys. Rev. A* **64**, 012706 (2001).
- [43] C. Mora and Y. Castin, *Phys. Rev. Lett.* **102**, 180404 (2009).
- [44] C. Cercignani, *The Boltzmann Equation and its Applications* (Springer, 1988).
- [45] The first three conditions ( $b(0) = 1$ ,  $\dot{b}(0) = 0$ ,  $\ddot{b}(0) = 0$ ) state the stationarity of  $\Psi(\mathbf{r}, t)$  for times  $t < 0$ . Conditions 4 and 5 ( $\dot{b}(t_f) = 0$ ,  $\ddot{b}(t_f) = 0$ ) state its stationarity for times  $t > t_f$ . Condition 6 follows from Eq. (6) and sets the final value of the scaling parameter ( $b(t_f) = (\omega_{01}/\omega_{f1})^{1/2}$ ).
- [46] C. Menotti, P. Pedri, and S. Stringari, *Phys. Rev. Lett.* **89**, 250402 (2002).
- [47] K. M. O'Hara, S. L. Hemmer, M. E. Gehm, S. R. Granade, and J. E. Thomas, *Science* **298**, 2179 (2002).
- [48] I. Brouzos, A. I. Streltsov, A. Negretti, R. S. Said, T. Canneva, S. Montangero, and T. Calarco, arXiv:1412.6142 (2014).
- [49] X. He, S. Yu, P. Xu, J. Wang, and M. Zhan, *Opt. Express* **20** (2012).